Title

Effect of Alzheimers Pathology on Task-Related Brain Network Reconfiguration in Aging.

Journal

Journal of Neuroscience, 43(38)

Authors

Jagust, William

Chen, Xi

Adams, Jenna

et al.

Publication Date

2023-09-20

DOI

10.1523/JNEUROSCI.0023-23.2023

Peer reviewed

Behavioral/Cognitive

Effect of Alzheimer's Pathology on Task-Related Brain Network Reconfiguration in Aging

Kaitlin E. Cassady,[1,2] Xi Chen,[1,2] Jenna N. Adams,[2] Theresa M. Harrison,[2] Kailin Zhuang,[2] Anne Maass,[3] Suzanne Baker,[1] and William Jagust[1,2]

[1]Molecular Biophysics and Integrated Bioimaging, Lawrence Berkeley National Laboratory, Berkeley, California 94720, [2]Helen Wills Neuroscience Institute, University of California Berkeley, Berkeley, California 94720, and [3]German Center for Neurodegenerative Disease, 39120 Magdeburg, Germany

Large-scale brain networks undergo widespread changes with older age and in neurodegenerative diseases such as Alzheimer's disease (AD). Research in young adults (YA) suggest that the underlying functional architecture of brain networks remains relatively consistent between rest and task states. However, it remains unclear whether the same is true in aging and to what extent any changes may be related to accumulation of AD pathology such as β-amyloid (Aβ) and tau. Here, we examined age-related differences in functional connectivity (FC) between rest and an object-scene mnemonic discrimination task using fMRI in young and older adults (OA; both females and males). We used an a priori episodic memory network (EMN) parcellation scheme associated with object and scene processing, that included anterior-temporal regions and posterior-medial regions. We also used positron emission topography to measure Aβ and tau in older adults. The correlation between rest and task FC (i.e., FC similarity) was reduced in older compared with younger adults. Older adults with lower FC similarity in EMN had higher levels of tau in the same EMN regions and performed worse during object, but not scene, trials during the fMRI task. These findings link AD pathology, particularly tau, to a less stable functional architecture in memory networks. They also suggest that smaller changes in FC organization between rest and task states may facilitate better performance in older age. Interpretations are limited by methodological factors related to different acquisition directions and durations between rest and task scans.

Key words: **aging; Alzheimer's disease; brain networks; functional connectivity; memory**

Significance Statement

The brain's large-scale network organization is relatively consistent between rest and task states in young adults (YA). We found that memory networks in older adults (OA) were less correlated between rest and (memory) task states compared with young adults. Older adults with less correlated brain networks also had higher levels of Alzheimer's disease (AD) pathology in the same regions, suggesting that a less stable network architecture may reflect the early evolution of AD. Older adults with less correlated brain networks also performed worse during the memory task suggesting that more similar network organization between rest and task states may facilitate better performance in older age.

Introduction

Functional connectivity (FC), the functionally integrated relationship between spatially distinct brain regions, reflects the brain's large-scale network organization. FC is typically examined during resting-state (i.e., task-free setting), but it can also be assessed while participants perform directed tasks. Research in young adults (YA) suggests that the underlying functional organization of brain networks remains relatively consistent between rest and task states (Cole et al., 2014). Furthermore, YA who exhibit relatively smaller changes in FC between rest and task states across several large-scale networks perform better on a range of cognitive domains (Schultz and Cole, 2016). Smaller FC changes between rest and task may reflect optimization for efficient network updates (Bullmore and Sporns, 2012). However, it remains unclear whether the same is true in aging, and to what extent any changes in FC organization between rest and task may be related to age-related cognitive decline. This is an important question because it raises the possibility that cognitive decline in some older adults (OA) may be attributed to dynamic changes in brain

Received Jan. 4, 2023; revised Aug. 2, 2023; accepted Aug. 6, 2023.

Author contributions: A.M. and W.J. designed research; A.M. performed research; K.E.C., X.C., J.N.A., T.M.H., K.Z., A.M., and S.B. analyzed data; K.E.C. and W.J. wrote the first draft of the paper; K.E.C., X.C., J.N.A., T.M.H., K.Z., A.M., S.B., and W.J. edited the paper; K.E.C., X.C., J.N.A., T.M.H., K.Z., A.M., S.B., and W.J. wrote the paper.

This work was supported by National Institutes of Health Grants AG034570 and AG067657. Avid Radiopharmaceuticals enabled the use of the ^{18}F-Flortaucipir tracer but did not provide direct funding and were not involved in data analysis or interpretation.

W.J. served as consultant for Biogen, Eisai, Lilly, and Bioclinica. All other authors declare no competing financial interests.

Correspondence should be addressed to Kaitlin Cassady at kcassady@berkeley.edu.

https://doi.org/10.1523/JNEUROSCI.0023-23.2023

network organization from rest to task demands, rather than dysfunction during either state alone (Hughes et al., 2020).

Decline in episodic memory is one of the hallmarks of age-related cognitive decline and is a major risk factor for dementia (Hedden and Gabrieli, 2004). Before the symptoms of dementia occur in Alzheimer's disease (AD), β-amyloid (Aβ) plaques and neurofibrillary tau tangles begin to appear in the brain. This process, particularly for tau, starts in the neural systems associated with episodic memory and tracks closely with cognitive decline (Nelson et al., 2012). The neural mechanisms underlying episodic memories combine information about objects/items and scenes/spatial context. Processing of these two types of information rely on distinct neural pathways in the neocortex and medial temporal lobe that converge in the hippocampus. Object processing involves an anterior-temporal (AT) system that includes fusiform gyrus/perirhinal cortex, inferior temporal gyrus, and amygdala. Scene processing relies on a posterior-medial system (PM) that includes retrosplenial cortex, precuneus, and parahippocampal cortex (Ranganath and Ritchey, 2012). Together, these regions work as an integrated episodic memory network (EMN) to support normal episodic memory.

Molecular and animal studies indicate that tau pathology spreads through brain regions via neural connections (de Calignon et al., 2012; Wu et al., 2016). Consistent with this, human neuroimaging studies indicate that FC between brain regions is predictive of the spatial pattern of tau pathology, as assessed by positron emission tomography (PET; Franzmeier et al., 2019; Vogel et al., 2020). Previous work by our group found that EMN in particular has distinct patterns of resting-state FC with entorhinal cortex subregions, and that such patterns predict the spatial topography and level of cortical tau deposition in cognitively normal OA (Adams et al., 2019). We also found that the modular functional organization of this EMN at rest was vulnerable to AD pathologies in OA (Cassady et al., 2021). However, few studies have investigated the relationship between task-based FC and AD pathology in brain networks, and to our knowledge, no previous studies have explored whether changes between rest and task FC in the EMN relate to the accumulation of AD pathology.

In this study, we first sought to compare resting-state to task-evoked FC during an object-scene mnemonic discrimination task to determine whether aging affects the consistency of the brain's episodic memory functional architecture during these two states. We hypothesized that FC between rest and task states would be less correlated in OA compared with YA. Second, we tested whether the magnitude of differences in FC between rest and task states was related to Aβ and tau pathology in OA. We hypothesized that less correlated rest versus task FC in the EMN would be associated with higher levels of tau pathology. Third, we tested whether FC differences between rest and task states were behaviorally relevant. We predicted that less correlated rest versus task FC would be related to worse task performance.

Materials and Methods

Participants

Young adults (YA; age range 20–35; 13 males, 11 females) and cognitively normal older adults (OA; age range 60–86; 18 males, 31 females) enrolled in the Berkeley Aging Cohort Study (BACS) participated in this study. All participants underwent structural and resting state fMRI (rsfMRI), as well as task-based fMRI while performing an object-scene mnemonic discrimination task (Berron et al., 2018; Maass et al., 2019). All OA additionally underwent tau-PET imaging using ^{18}F-Flortaucipir (FTP), Aβ-PET with ^{11}C-Pittsburgh Compound-B (PiB), and a standard neuropsychological assessment. Inclusion criteria for participants required a Mini-Mental State Exam (MMSE) score of $\geq$25 and neuropsychological scores within 1.5 SDs of age, education and sex adjusted norms. We excluded any participants with a history of significant neurologic disease (e.g., stroke, seizure, or loss of consciousness $\geq$10 min), or any medical illness that could affect cognition. We also excluded participants with a history of substance abuse, depression, and contraindications to MRI or PET. All study procedures were reviewed and approved by the Institutional Review Boards of the University of California Berkeley and Lawrence Berkeley National Laboratory (LBNL). All participants provided detailed written consent for their involvement in this study. Demographic information for each age group is presented in Table 1.

Table 1. Cohort demographics

	YA ($n = 24$)	OA ($n = 49$)
Age	26.5 ± 4.3 (20–35)	73.7 ± 5.1 (60–86)
Sex (M/F)	13/11	18/31
Education (years)	16.7 ± 2.4	16.7 ± 1.8
MMSE	29.4 ± 0.81	28.5 ± 1.2
APOE ε4 (C/NC)	N/A	16/33
Global PiB DVR	N/A	1.15 ± 0.22 (0.97–1.89)
EMN FTP SUVR	N/A	1.2 ± 0.13 (0.96–1.6)
PiB+/−	N/A	22/27
Motion (FD)	0.11 ± 0.09	0.18 ± 0.09

MMSE = Mini-Mental State Exam; C/NC = Carrier/Noncarrier; PiB = ^{11}C-Pittsburgh Compound-B; EMN = Episodic Memory Network; FTP = ^{18}F-Flortaucipir; DVR = Distribution Volume Ratio; SUVR = Standard Uptake Value Ratio; YA = Young Adults; OA = Older Adults; FD = framewise displacement.

Functional and structural MRI

3T MRI acquisition

All participants underwent structural and functional MRI which was acquired on a 3T TIM/Trio scanner (Siemens Medical System, software version B17A) using a 32-channel head coil. High-resolution whole brain structural images were acquired using a T1-weighted volumetric magnetization prepared rapid gradient echo (GE) image (MPRAGE; voxel size = 1 mm isotropic, TR = 2300 ms, TE = 2.98 ms, matrix = 256 × 240 × 160, FOV = 256 × 240 × 160 mm^3, sagittal plane, 160 slices, 5-min acquisition time).

This was followed by a rsfMRI scan that was acquired using T2*-weighted echoplanar imaging (EPI) with the following parameters: voxel size = 2.6 mm isotropic, TR = 1067 ms, TE = 31.2 ms, FA = 45, matrix = 80 × 80, FOV = 210 mm, sagittal plane, 300 volumes, anterior to posterior phase encoding, ascending acquisition, 5-min acquisition time. During the rsfMRI scan, participants were instructed to remain awake with their eyes open and focused on the screen, which displayed a white asterisk on a black background.

FMRI was then acquired while participants performed an object-scene mnemonic discrimination task. High-resolution whole-brain functional data were acquired using T2*-weighted gradient echo (GE) EPI, with the following parameters: voxel size 1.54 mm isotropic, multiband acceleration factor 4, TR = 2400 ms, TE = 37 ms, flip angle = 45, matrix = 138 × 138, FOV = 212 × 212 mm^2, interleaved acquisition, 88 slices, PA phase encoding, two 13 min runs. Two gradient echo images with different echo times were also collected to create a phase map for distortion correction, with the following parameters: 1.54-mm isotropic resolution, R-L encoding direction, TR = 1000 ms, flip angle = 60, TE1 = 5.6 ms, TE2 = 8.06 ms.

1.5T MRI acquisition and processing

Structural MRI data were acquired for standard PET processing at LBNL. A whole-brain high-resolution T1-weighted volumetric MPRAGE was acquired on a 1.5T Siemens Magnetome Avanto scanner (Siemens, Inc; 1-mm isotropic voxels, TR = 2110 ms, TE = 3.58 ms, FA = 15). These structural MRIs were used for PET coregistration and were segmented using FreeSurfer v.5.3.0 (http://surfer.nmr.mgh.harvard.edu/) to derive native space regions of interest (ROIs) for FTP and PiB quantification.

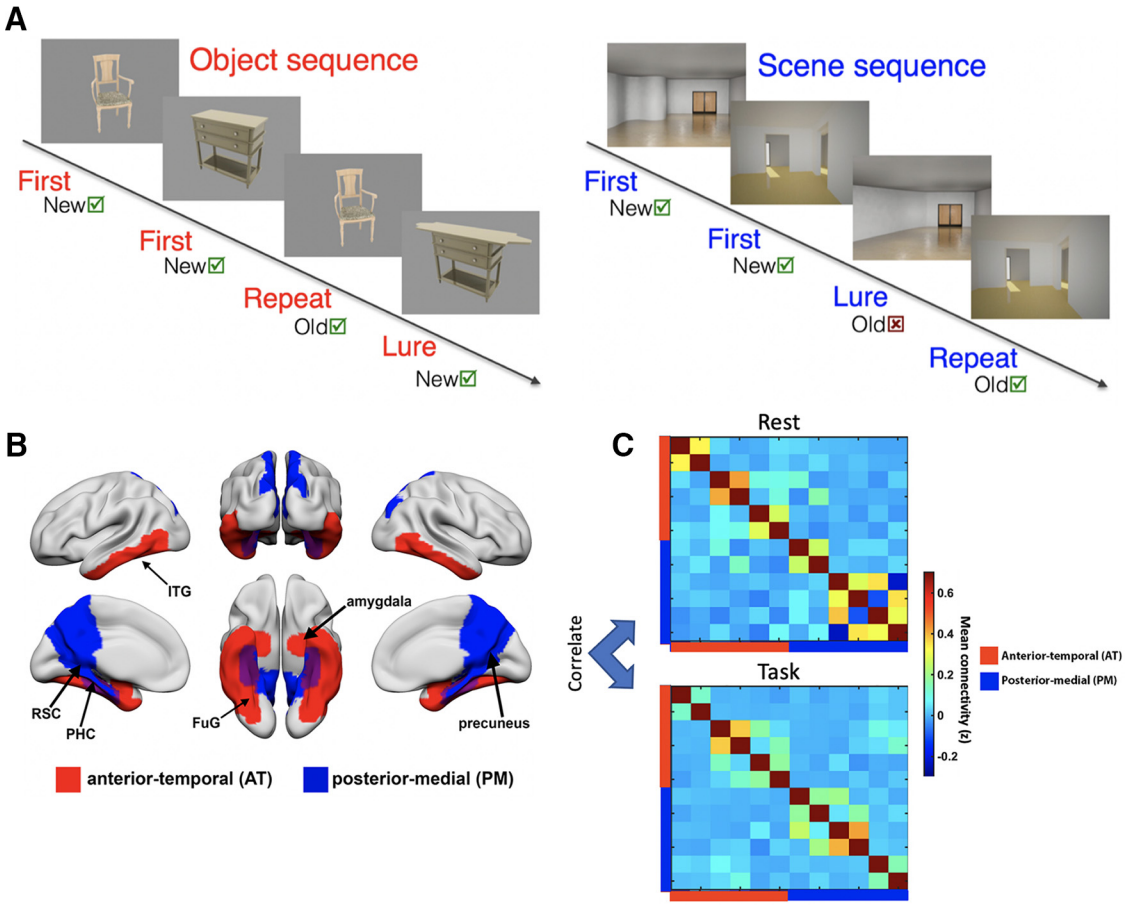

Figure 1. Visual representation of the fMRI task, regions comprising the episodic memory network (EMN), and the calculation of functional connectivity (FC) similarity. ***A***, All participants performed an object-scene mnemonic discrimination task during fMRI acquisition. The first two stimuli of each block were novel stimuli, whereas the second two stimuli were either identically repeated or highly similar lure stimuli. Participants were instructed to respond "old" or "new" to each stimulus. ***B***, Regions of interest in anterior-temporal (AT; red) and posterior-medial (PM; blue) that comprised the EMN. These regions included amygdala, fusiform gyrus (FuG)/perirhinal cortex, inferior temporal gyrus (ITG), retrosplenial cortex (RSC), precuneus, and parahippocampal cortex (PHC). ***C***, The correlation of FC between rest and task states (i.e., FC similarity) was calculated by conducting a Pearson's correlation between the rest and task ROI-to-ROI matrices for each participant.

fMRI task

During the fMRI scan, participants performed a continuous recognition memory task on objects and scenes (Fig. 1*A*). This task is described in detail in Berron et al. (2018). Participants were visually presented with blocks of either four object or scene stimuli, in which the first two stimuli in each block were novel, and the second two stimuli were either repeated (correct response: "old"; hit) or followed by a highly similar "lure" (correct response: "new"; correct rejection). The task was divided into two 13 min runs, each starting and ending with 10 "scrambled noise" images with a similar luminance and color to the task stimuli. Participants were instructed to press the "new" button for all noise images in the beginning and the "old" button at the end of the task. These images served as the "perceptual" baseline condition for subsequent fMRI analyses. Task stimuli were presented in an event-related design using Neurobehavioral Systems (http://nbs.neurobs.com). Stimuli were presented for 3 s separated by a white fixation star using jittered interstimulus intervals ranging from 0.6s to 4.2 s. Intervals between sequences were longer (mean of 2.43 s) to emphasize the end of a sequence. There were 128 sequences consisting of four stimuli with 32 first-repeat pairs and 32 first-lure pairs per (object/scene) domain (256 trials total). Lure images were produced by changing local features of the objects (i.e., shape) and global features of the rooms (i.e., geometry). Before scanning, participants were verbally instructed and shown a standardized visual instruction with all information regarding the task. After this, they had to learn the task within a 2-min training run outside of the scanner. During this training session, a standard vision screening procedure and a visual discrimination test with comparable stimuli to those used in the experiment were conducted to rule of potential confounding effects of deficits in visual acuity. Vision was corrected using MR-compatible devices if necessary. As a measure of behavioral performance, we calculated proportion correct for lures (correct rejection rate = 1 – false alarm rate) during object and scene conditions. We used lure conditions since these measures are most sensitive to AD pathology (Maass et al., 2019) and they did not suffer from ceiling effects as some of the other behavioral measures did (i.e., hit rates).

fMRI preprocessing

rsfMRI and task-based fMRI data were preprocessed identically, except where noted, for consistency. Preprocessing was performed using Statistical Parametric Mapping (SPM, version 12, Wellcome Trust Centre for Neuroimaging, London, UK). Preprocessing steps included slice time correction, realignment, coregistration to the T1 structural image, and outlier volume detection. For distortion correction (for the task data), we used the Fieldmap toolbox (v2.1) and the "Realign and Unwarp" module in SPM12. First, a voxel displacement map (vdm) was created using the Fieldmap toolbox by presubstraction of phase and magnitude images. During that process, the anatomic T1 image was co-registered to the first EPI. Next, the combined effects of static and movement-related susceptibility-induced distortions were calculated and corrected for using the "Realign and Unwarp" module. Outliers in the average signal intensity and scan-to-scan motion were identified using the Artifact Detection Toolbox (ART; http://www.nitrc.org/projects/artifact_detect) using a conservative threshold of >0.5 mm/TR and a global signal intensity z score of 3 (Lemieux et al., 2007; Power et al., 2014). These outlier volumes were flagged and included as spike

regressors during the denoising procedure (Lemieux et al., 2007; Power et al., 2014) using the CONN toolbox (v18a; www.nitrc.org/projects/conn). Additional denoising on the fMRI data were conducted in preparation for FC analyses using CONN. First, temporal and confounding factors were regressed from each voxel BOLD timeseries and the resulting residual timeseries were filtered using temporal band or high-pass filters to examine the frequency bands of interest and to exclude higher frequency sources of noise such as heart rate and respiration. The rsfMRI data were filtered using a temporal band filter of 0.008–0.09 Hz, whereas the task-based fMRI data were filtered using a temporal high-pass filter of 0.008 Hz. This filter was used for the task-based data to avoid unnecessary smoothing over task boundaries. In addition, for task-based data only we conducted a general linear model (GLM) regression of task events and used the residuals to compute FC. This additional step limits the spurious inflation of FC estimates by task activations, allowing us to conclude that state differences in FC were not because of task-related global changes in neural activity (Cole et al., 2019). For additional noise reduction, we used the anatomic component-based noise correction method, aCompCor (Behzadi et al., 2007). Residual head movement parameters (three rotations, three translations, and six parameters representing their first-order temporal derivatives) and signals from white matter (WM) and CSF, and spike regressors from motion detection were regressed out during the computation of FC maps.

fMRI first-level analysis

First-level ROI-to-ROI analysis was performed using the CONN toolbox. As described in previous studies from our lab (Maass et al., 2019; Cassady et al., 2021; Chen et al., 2021), we used 12 FreeSurfer ROIs that included bilateral amygdala, fusiform gyrus (FuG)/perirhinal cortex, inferior temporal gyrus, retrosplenial cortex (RSC), parahippocampal cortex (PHC), and precuneus, which together formed our integrated EMN (Fig. 1*B*). Semi-partial correlations were computed for these first-level analyses to determine the unique variance of each (unilateral) seed, controlling for the variance of all other seed regions that were entered into the same model. For each participant, the BOLD time series within each of the ROIs was extracted and the mean time series was computed. Then, the cross-correlation of each ROI's time course with every other ROI's time course was computed, creating a 12×12 correlation matrix for each participant. Correlation coefficients were converted to z-values using Fisher's r-to-z transformation (Zar, 1996), and the diagonal of each matrix was removed. For this study, we collapsed our analyses of task FC across all object and scene conditions to limit the number of statistical comparisons and to achieve the highest power. Thus, each participant had one resting state FC matrix and one task-related FC matrix that was averaged across all task conditions (including first, lure, and repeat trials). We then determined the correlation of FC between rest and task states (i.e., FC similarity) by conducting a Pearson's correlation between the rest and task ROI-to-ROI matrices for each participant (Schultz and Cole, 2016; Hughes et al., 2020; Fig. 1*C*).

Reduced FC similarity in OA may occur because the modular organization of their networks changes between rest and task states to a greater extent than in younger adults. To test this follow-up hypothesis, we calculated a graph measure of functional network organization, segregation, specifically of object-specialized and scene-specialized components of the EMN. We measured segregation during both rest and task states for each participant. Network segregation was calculated as the difference in mean within-network FC and mean between-network FC divided by mean within-network FC:

$$\text{Network segregation} = \frac{\bar{Z}_w - \bar{Z}_b}{\bar{Z}_w},$$

where $\bar{Z}_w$ is the mean Fisher z-transformed correlation between ROIs within the same subnetwork (e.g., AT) and $\bar{Z}_b$ is the mean Fisher z-transformed correlation between ROIs of one network with all ROIs in the other subnetwork (e.g., PM; Chan et al., 2014). Segregation was averaged between AT and PM subnetworks as our final measures of segregation for each state and each participant.

PET

PET acquisition

OA participants underwent PET scanning at LBNL using a Biograph PET/CT Truepoint 6 scanner (Siemens). CT scans were conducted for attenuation correction before each emission acquisition and radiotracers were synthesized at the LBNL Biomedical Isotope Facility. Pathologic tau aggregation was measured using ^{18}F-Flortacipir (FTP) with data binned into 4×5 min frames from 80–100 min postinjection (Maass et al., 2017; Adams et al., 2019; Harrison et al., 2019). Aβ was measured using ^{11}C-Pittsburgh Compound-B (PiB), with data acquired across 35 dynamic frames for 90 min postinjection (4×15, 8×30, 9×60, 2×180, 10×300, and 2×600 s). All PET images were reconstructed using an ordered subset expectation maximization algorithm, with attenuation correction, scatter correction, and smoothing using a Gaussian kernel of 4 mm.

PET preprocessing

As mentioned above, 1.5T structural MRI data were preprocessed with FreeSurfer (version 7.1.0) to acquire ROIs in participant native space. Both FTP and PiB images were preprocessed using SPM12. FTP images were first realigned, then averaged, and coregistered to each participant's 1.5T structural scan. Standardized uptake value ratio (SUVR) values were computed by averaging the mean tracer uptake over the 80- to 100-min data and normalized by an inferior cerebellar gray reference region (Baker et al., 2017a). The mean SUVR of each (FreeSurfer segmented) ROI was extracted from the native space images. This data were then partial volume corrected using a modified Geometric Transfer Matrix approach (Rousset et al., 1998) as previously described (Baker et al., 2017b). The weighted mean (by region size), partial volume corrected FTP SUVR of all 12 EMN ROIs was used in subsequent analyses.

PiB images were realigned, averaged across frames from the first 20 min of acquisition which was then used to derive the coregistration matrix to move the individual PiB frames to each participant's 1.5T structural MRI image. DVR values were calculated for the PiB-PET images using Logan graphical analysis over 35–90 min with a cerebellar gray matter (GM) reference region (Logan et al., 1996). PiB DVR values are typically calculated using a global measure because different cortical regions across the brain are highly correlated. Thus, global PiB DVR values were calculated across multiple cortical ROIs as previously detailed (Mormino et al., 2012), and a threshold of 1.065 DVR was used to classify participants into A$\beta+$ and A$\beta-$ groups (Villeneuve et al., 2015). One participant was missing PiB data and therefore excluded from all PiB analyses.

Experimental design and statistical analyses

Statistical analyses were performed using R (http://www.R-project.org/) and SPSS (SPSS Inc; version 27.0.1.0) software. Independent sample t tests were used to examine age group differences in FC similarity. Multiple regression models were used to examine the relationship between FC similarity, network segregation, PiB and FTP, and task performance. All statistical models were adjusted for age, sex, motion, GM volume (in EMN ROIs), and for models including cognitive measures, years of education. We used a two-tailed level of $p < 0.05$ for determining statistical significance.

Results

FC similarity is reduced with older age

Our first aim was to determine whether FC similarity (i.e., the correlation between rest and task FC states in the EMN) was significantly different between OA and YA. Figure 2*A* displays the correlation matrices for each age group during each state (rest and task). Replicating previous studies (i.e., Hughes et al., 2020), OA exhibited lower FC similarity between rest and task states compared with younger adults ($t_{(69)} = 6$, $p < 0.001$, $d = 1.5$; Fig. 2*B*). GM volume did not affect this relationship when we included it as a nuisance regressor in a partial correlation analysis ($r_{(68)} = -0.61$, $p < 0.001$).

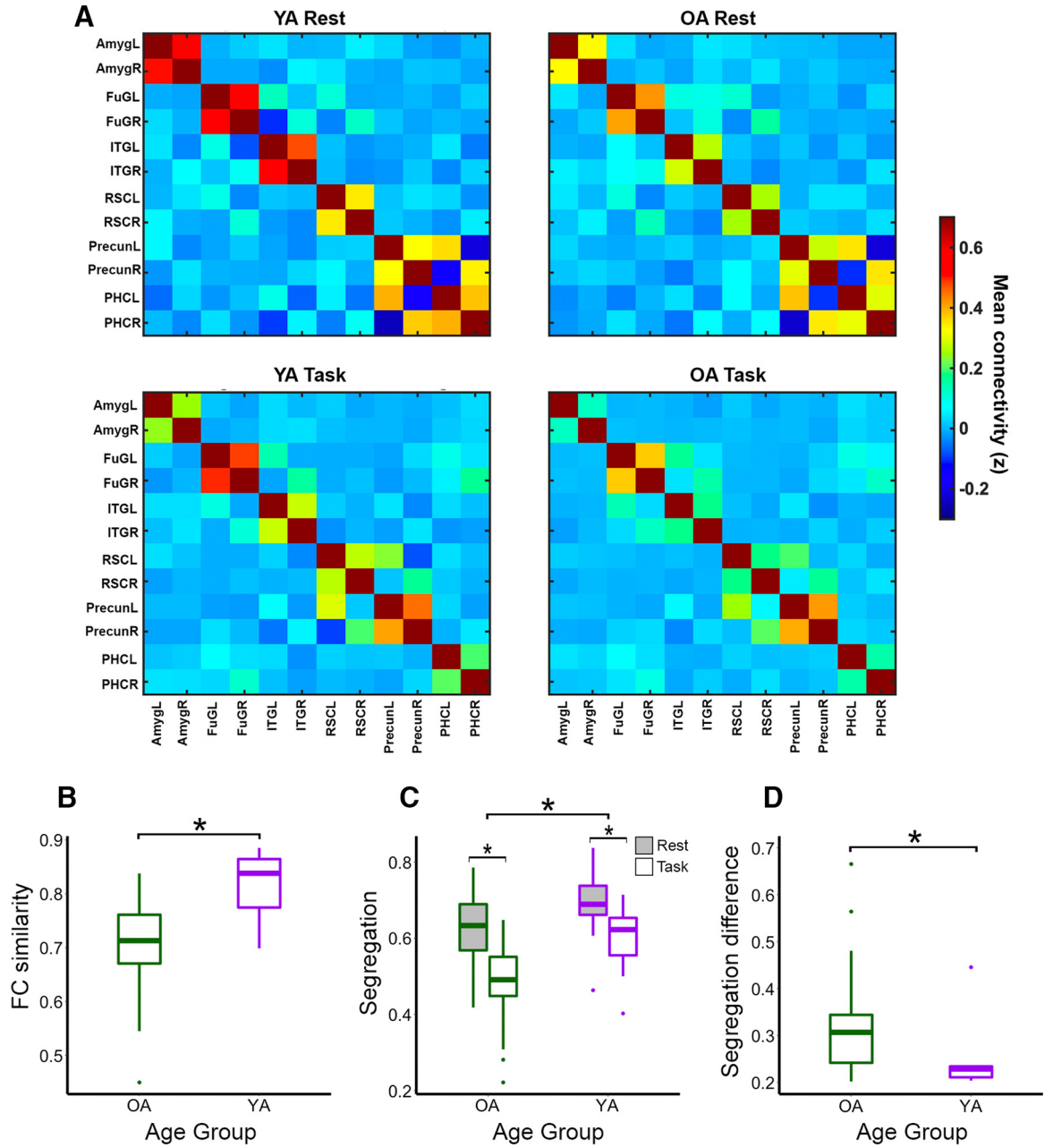

Figure 2. Functional connectivity (FC) similarity is reduced in older compared with younger adults and the segregation of older adults' episodic memory networks changes between rest and task states to a greater degree in older than in younger adults. ***A***, Region of interest (ROI) i.e., ROI-to-ROI correlation matrices for each age group during each state (rest and task). ***B***, Independent samples *t* test indicated that older adults (green) have lower FC similarity compared with younger adults (purple). ***C***, Repeated measures ANOVA showed a main effect of FC state such that both age groups exhibited higher segregation during rest (gray) compared with task (white) states. They also showed a main effect of age group such that younger adults exhibited higher segregation during both rest and task states compared with older adults. ***D***, Older adults showed a greater difference in rest versus task segregation compared with younger adults. On each box, the central mark indicates the median, and the bottom and top edges of the box indicate the 25th and 75th percentiles, respectively. The whiskers extend to the most extreme data points not considered outliers.

As a follow-up analysis to test which regions influenced these age differences, we calculated FC similarity between rest versus task using specific regional connections (e.g., amygdala to FuG, amygdala to ITG, amygdala to RSC, etc.) as well the average FC within AT and PM networks. Using *t* tests to test for age differences, we found significant age differences in FC similarity within AT networks ($t_{(69)} = 4.8$, $p < 0.001$, $d = 1.2$) and PM networks ($t_{(69)} = 3.2$, $p = 0.002$, $d = 0.83$), in addition to specific connections between precuneus and PHC ($t_{(69)} = 2.1$, $p = 0.037$, $d = 0.55$). That is, YA showed a higher correlation between rest and task FC specifically within these ROIs/networks compared with OA.

Reduced FC similarity in OA may occur because the modular organization of their networks changes between rest and task states to a greater extent than in younger adults. To test this, we calculated network segregation during both rest and task states for each participant. We then performed a mixed measures ANOVA using "FC state" (i.e., rest or task segregation) as a within-subject factor and age group as a between-subject factor. We observed a significant main effect of FC state such that both age groups exhibited higher segregation during rest compared with task states ($F_{(1,69)} = 31.5$, $p < 0.001$, $\eta p^2 = 0.48$). We also observed a main effect of age group such that YA exhibited higher segregation during both rest and task states compared

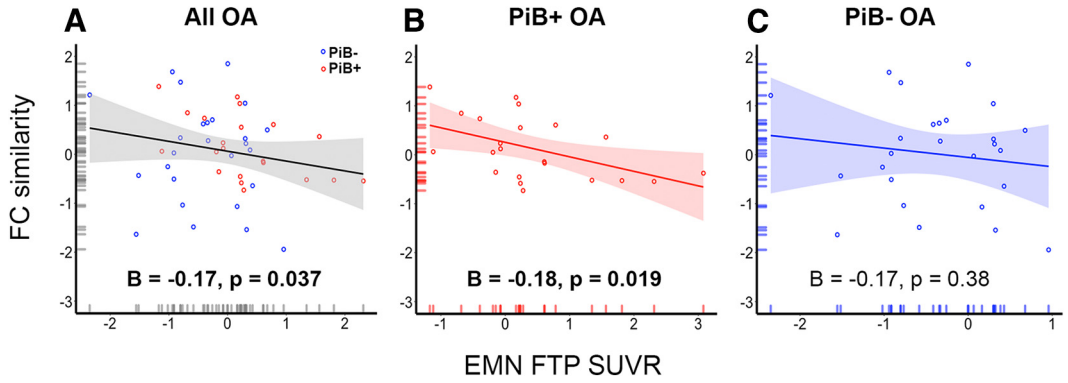

Figure 3. Higher levels of tau pathology in episodic memory network regions predict lower functional connectivity (FC) similarity. Multiple regression analyses indicated that higher levels of tau in the episodic memory network (EMN) regions are associated with lower FC similarity across (***A***) all older adults and (***B***) in PiB+ older adults only, but (***C***) not in PiB− older adults only. Blue data points reflect PiB− older adults, whereas red data points reflect PiB+ older adults. PiB = 11C-Pittsburgh Compound-B.

Table 2. Multiple regression results for EMN FTP SUVR predicting FC similarity

	All OA		PiB+ OA		PiB− OA	
Predictor	*B*	*p*	*B*	*p*	*B*	*p*
Age	−0.003	0.14	−0.003	0.29	−0.003	0.29
Sex	−0.009	0.66	0.019	0.39	−0.065	0.14
PiB-status	0.026	0.27	N/A	N/A	N/A	N/A
Motion	−0.3	0.11	−0.087	0.51	−0.79	0.05
EMN FTP SUVR	−0.18	0.041	−0.17	0.015	−0.39	0.11
GM volume	−7.90E-07	0.51	−1.29E-06	0.37	−6.42E-07	0.74

PiB = 11C-Pittsburgh Compound-B; EMN = episodic memory network; GM = gray matter; FTP = 18F-Flortaucipir; DVR = Distribution Volume Ratio; SUVR = Standard Uptake Value Ratio.

with OA ($F_{(1,69)} = 27.4$, $p < 0.001$, $\eta p^2 = 0.28$; Fig. 2*C*). The interaction between FC state and age group was not significant, although it was in the expected direction ($F_{(1,69)} = 2$, $p = 0.16$, $\eta p^2 = 0.031$) where the FC segregation decrease from rest to task state appeared to be larger in OA than YA.

To test whether the relative difference between rest and task segregation was greater in OA compared with YA using a novel normalized difference metric, we measured the absolute value of the difference between rest and task segregation divided by rest segregation. We then performed an independent sample *t* test between the two age groups. As expected, OA exhibited a significantly greater difference in rest versus task segregation compared with YA ($t_{(69)} = 2.3$, $p = 0.025$, $d = 0.59$; Fig. 2*D*). This indicates that age-related dedifferentiation of AT/PM networks during rest becomes even more exacerbated during this recognition memory task.

Higher levels of tau pathology predict lower FC similarity

Our second aim was to examine the relationship between AD pathology (Aβ and tau) and FC similarity. To assess these relationships, we performed multiple regression models including age, sex, PiB-status and EMN FTP on FC similarity. Neither PiB-status ($B = 0.04$, $p = 0.15$, $r^2 = 0.071$) nor global PiB ($B = -0.06$, $p = 0.16$, $r^2 = 0.071$) were associated with FC similarity. However, higher levels of FTP in the EMN predicted lower FC similarity. Intriguingly, this relationship was observed across all OA [including both PiB− and PiB+ groups ($B = -0.17$, $p = 0.037$, $r^2 = 0.12$; Fig. 3*A*)] as well as in the PiB+ group alone ($B = -0.18$, $p = 0.019$, $r^2 = 0.34$; Fig. 3*B*). However, there was not a significant relationship in the PiB− group alone ($B = -0.17$, $p = 0.38$, $r^2 = 0.066$; Fig. 3*C*). There was no interaction between PiB-status (or global PiB) and EMN FTP on FC similarity ($ps > 0.36$). Table 2 reports the results of these regressions. These findings indicate that AD pathology is linked to a less consistent functional architecture of the EMN during rest compared with task states.

Higher FC similarity is associated with better performance during object, but not scene, trials

Our third aim was to explore the relationship between FC similarity and task performance. Specifically, we used proportion correct (i.e., correct rejection) during object and scene lure trials as our measures of task performance. To assess these relationships between FC similarity with performance, we conducted multiple regression models including age, sex, education, and FC similarity predicting to proportion correct on object and scene lure trials separately. We found that higher FC similarity was related to a higher proportion correct during object lure trials. This was observed across all subjects [including OA and YA ($B = 0.64$, $p = 0.02$, $r^2 = 0.27$; Fig. 4*A*)] as well as OA alone ($B = 0.77$, $p = 0.037$, $r^2 = 0.22$; Fig. 4*B*). However, there was not a significant relationship between FC similarity and performance in YA alone ($B = -0.01$, $p = 0.99$, $r^2 = 0.18$; Fig. 4*C*). FC similarity was not associated with performance during scene lure trials in any group (all $ps > 0.53$; Figs. 4*D–F*). Tables 3 and 4 report the results of these regressions. Neither PiB nor EMN FTP were associated with performance, all $ps > 0.31$.

Control analysis

As a control analysis, we tested whether the relationships between FC similarity with age, AD pathology and task performance were specific to the EMN or showed a more global (i.e., whole brain) effect. To that end, we performed the same processing and analysis procedures as described above except we calculated FC similarity using a whole-brain (FreeSurfer) 264-ROI parcellation scheme based on the Brainnetome atlas (Fan et al., 2016) and categorized into seven canonical networks based on the Yeo parcellation scheme (Thomas Yeo et al., 2011). As described above, we calculated the correlation of FC between rest and task states (i.e., FC similarity) by conducting a bivariate Pearson's correlation between the rest and task ROI-to-ROI matrices for each participant.

We first tested whether there were significant age group differences in whole-brain FC similarity by performing an independent sample *t* test. Figure 5*A* displays the correlation matrices for each age group during each state (rest and task). We found that OA exhibited lower FC similarity between rest and task states compared with younger adults ($t_{(69)} = 7.7$, $p < 0.001$, $d = 1.4$; Fig. 5*B*). As a follow-up analysis to test which networks

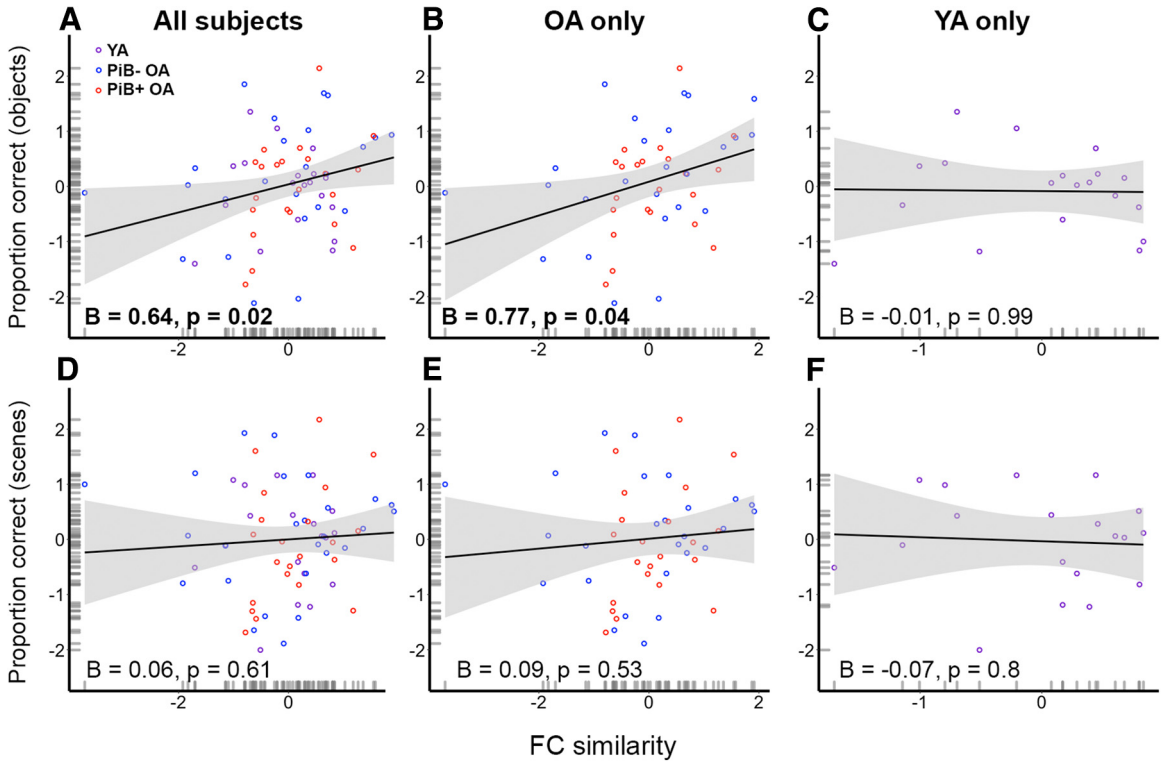

Figure 4. Higher functional connectivity (FC) similarity is associated with better task performance during object, but not scene trials. Multiple regression analyses showed that higher FC similarity was associated with a higher proportion correct during object lure trials (***A***) across all subjects and (***B***) in the older adult group alone, but (***C***) not in the younger adult group alone. FC similarity was not associated with performance during scene lure trials. This was the case (***D***) across all subjects, (***E***) in the older adult group alone, and (***F***) in the younger adult group alone. Blue data points reflect PiB− older adults whereas red data points reflect PiB+ older adults. Purple data points reflect young adults.

Table 3. Multiple regression results for FC similarity predicting proportion correct during object lures

	All subjects		OA		YA	
Predictor	*B*	*p*	*B*	*p*	*B*	*p*
Age	−0.003	0.027	−0.01	0.11	−0.021	0.03
Sex	0.035	0.41	0.08	0.11	−0.018	0.75
Education	0.007	0.5	0.01	0.46	0.007	0.6
Motion	−0.06	0.81	0.33	0.45	−1.02	0.03
FC similarity	0.62	0.029	0.84	0.021	−1.1	0.15
GM volume	−2.78E-06	0.2	−3.96E-06	0.12	−1.41E-07	0.97

FC = functional connectivity; GM = gray matter.

Table 4. Multiple regression results for FC similarity predicting proportion correct during scene lures

	All subjects		OA		YA	
Predictor	*B*	*p*	*B*	*p*	*B*	*p*
Age	−0.004	0.008	−0.008	0.27	−0.012	0.43
Sex	0.005	0.92	0.04	0.56	−0.05	0.69
Education	0.006	0.65	0.008	0.55	0	0.98
Motion	−0.17	0.5	0.014	0.98	−0.62	0.35
FC similarity	0.12	0.74	0.26	0.52	−0.7	0.55
GM volume	−2.10E-06	0.43	−3.50E-06	0.3	2.30E-06	0.69

FC = functional connectivity; GM = gray matter.

influenced these age differences, we calculated FC similarity between rest versus task in all seven canonical networks. Using *t* tests to test for age differences, we found significant age differences in FC in all networks except for the dorsal attention network. That is, YA showed a higher correlation between rest and task FC specifically within these networks compared with OA.

We also calculated global measures of segregation during both rest and task states for each participant and performed a mixed measures ANOVA using "FC state" (i.e., rest or task segregation) as a within-subject factor and age group as a between-subject factor. Similar to the local EMN segregation results, we observed a main effect of age group such that YA exhibited higher segregation during both rest and task states compared with OA ($F_{(1,69)} = 34$, $p < 0.001$, $\eta p^2 = 0.33$). In contrast to the local EMN segregation results, we observed a main effect of FC state such that both age groups showed higher segregation during *task* compared with *rest* states ($F_{(1,69)} = 25.7$, $p < 0.001$, $\eta p^2 = 0.27$). The interaction between FC state and age group was significant, although in the opposite direction from the EMN results ($F_{(1,69)} = 6.1$, $p = 0.02$, $\eta p^2 = 0.082$); in this case, the FC segregation decrease from task to rest state was larger in YA compared with OA (Fig. 5*F*,*G*).

We next examined the relationship between whole-brain FC similarity and AD pathology. We did not observe any significant associations between FC similarity with either PiB-status (or global PiB; all $ps > 0.67$) or EMN FTP ($B = 0.008$, $p = 0.84$, $r^2 = 0.073$; Fig. 5*C*). Finally, we tested whether whole-brain FC similarity was associated with task performance. We did not observe any significant associations between FC similarity and task performance during either object ($B = -0.02$, $p = 0.97$, $r^2 = 0.21$; Fig. 5*D*) or scene lure trials ($B = -0.35$, $p = 0.67$, $r^2 = 0.2$; Fig. 5*E*). These results indicate that although the effects of age on FC similarity may represent a more global (brain-wide) phenomenon, the link between FC similarity with AD pathology, and object-related memory ability may reflect more local effects confined to the EMN.

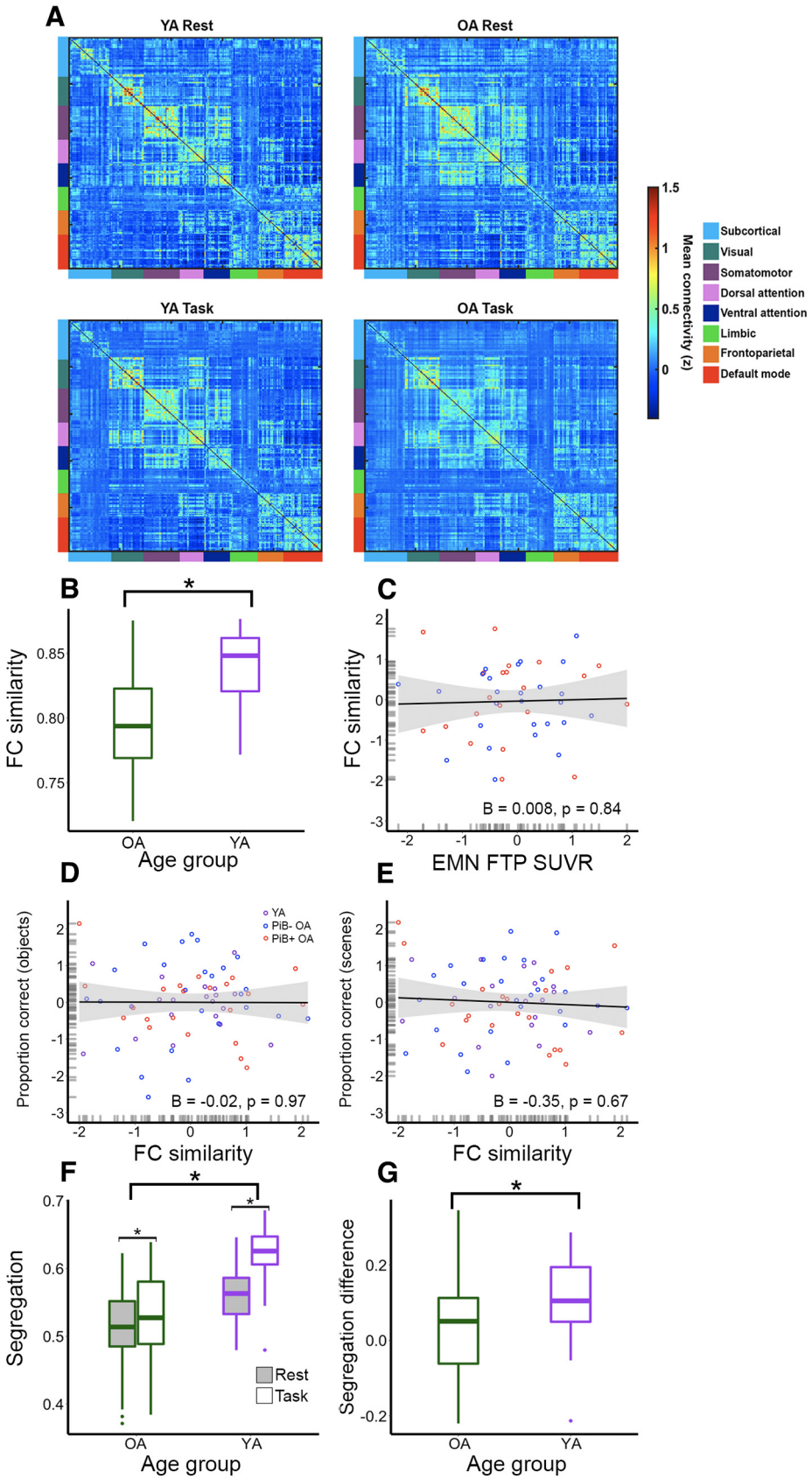

Figure 5. Control analyses using a whole-brain Brainnetome parcellation scheme partitioned into Yeo's seven canonical networks. ***A***, Region of interest (ROI-to-ROI) correlation matrices for each age group during each state (rest and task). ***B***, Independent samples *t* test indicated that older adults have lower global functional connectivity (FC) similarity compared with younger adults. ***C***, Multiple regression analyses showed that FTP SUVR levels in EMN regions were not associated with global FC similarity. Multiple regression analyses showed that FC similarity was not associated with task performance, either during (***D***) object or (***E***) scene lure trials. ***F***, Repeated measures ANOVA showed a main effect of FC state such that both age groups exhibited higher segregation during task (white) compared with rest (gray) states. They also showed a main effect of age group such that younger adults exhibited higher segregation during both rest and task states compared

Discussion

The main goal of this study was to investigate the effects of age and AD pathology on task-related reconfiguration of the networks supporting episodic memory. We also tested whether FC differences between rest and task states were related to task performance. OA showed reduced FC similarity between rest and task states compared with YA. An explanation for this effect is that OA's less segregated networks during resting state were further dedifferentiated during the task. Higher levels of tau in the EMN regions were associated with lower FC similarity in OA. This effect was driven by Aβ + OA, linking AD pathology to a weaker functional architecture of these memory-related networks. Higher FC similarity was associated with better task performance during object, but not scene, trials in OA indicating greater associations between EMN network configuration and object trials. Consistent with the reconfiguration hypothesis, these results suggest that smaller changes in FC organization between rest and task states in the EMN may facilitate better performance in older age.

FC similarity declines with age

We found that age was associated with changes in the stability of functional network architecture during rest versus task states. This finding is consistent with previous studies showing age differences in FC organization between rest and task states during sensorimotor (Monteiro et al., 2019) and reasoning judgment (Hughes et al., 2020) tasks. Whereas these previous studies explored the whole-brain organization of canonical resting state networks, we demonstrated robust age effects in the EMN, a network vulnerable to AD pathology and episodic memory decline. A loss of episodic memory is one of the hallmarks of age-related cognitive decline and is an early symptom of AD (Hedden and Gabrieli, 2004). By studying this episodic memory system in healthy OA and its association with AD pathology, we can advance our understanding of healthy aging and the progression from healthy to pathologic aging, which could serve as a crucial building block for the early detection of AD.

In addition to showing age differences in FC similarity in the EMN, we also demonstrated a potential explanation for this effect. OA showed a significantly greater difference between rest and task segregation in the EMN compared with YA. Thus, a lower correlation between rest and task states in older compared with YA may arise because the organization of OA's EMN networks changes between states to a greater degree. This pattern of less segregation between networks in response to a task is consistent with previous studies in YA (Cohen and D'Esposito, 2016; Shine et al., 2016). However, the present finding that OA showed a significantly greater difference in rest versus task segregation in EMN compared with YA raises the possibility that aging disproportionately affects FC in the EMN in one state (task) compared with the other (rest). This likely disrupts how brain networks interact in a way that is detrimental for cognition.

AD pathology relates to FC similarity

We found that higher levels of tau in EMN regions were associated with reduced FC similarity in OA. This relationship was driven by OA with higher levels of Aβ, linking AD pathology to a less stable network architecture during rest versus task states. Although much previous work has linked Aβ and tau pathology with intrinsic network connectivity (Adams et al., 2019; Berron et al., 2020; Cassady et al., 2021), no studies, to our knowledge, have investigated the relationship between these pathologies with the dynamic changes in FC during different cognitive states. This is important because state-dependent changes to functional connections play a crucial role in dynamically reshaping brain network organization. In the aggregate, these findings suggest that as tau pathology accumulates through the brain along neural connections it interferes with network function both during rest and task states.

FC similarity is associated with task performance

We found that higher FC similarity was associated with better performance during object trials. This is in line with previous studies that have demonstrated a positive correlation between FC similarity and cognitive performance in YA (Schultz and Cole, 2016). Consistent with the neural efficiency hypothesis, these findings suggest that smaller changes in FC organization between different task states may facilitate better performance in older age. Previous work supports the possibility that better performance is related to efficient neural processing. For instance, individuals with higher intelligence scores show less metabolic brain activity during task performance (Haier et al., 1988). We expand on these results in the current study by showing that FC reconfiguration between rest and (memory) task states is related to performance. This suggests that the neural efficiency hypothesis applies to both task-evoked BOLD responses and to the efficiency by which FC patterns reconfigure to different task demands.

FC alterations were specifically related to older adults' performance during object, but not scene, trials. This suggests that age-related memory impairments that are disproportionate across information domains may be related to less efficient network reconfigurations. Our results are consistent with previous studies demonstrating a greater loss of object compared with spatial mnemonic discrimination in cognitively normal OA (Reagh et al., 2016; Berron et al., 2018). Previous studies have demonstrated selective targeting of early age-related and Alzheimer's related neurodegeneration to specific regions of the brain. In particular, the perirhinal and lateral entorhinal cortices, key regions in the EMN thought to process object/item information, are among the earliest functional and anatomic targets of tau pathology (Burke et al., 2011; Yassa, 2014). These brain regions are also the earliest to show pathologic tau accumulation. The current findings indicate that dysfunction in these brain regions is in fact related to tau, specifically potentiated by Aβ. This suggests that loss of FC similarity may reflect the early evolution of AD.

Control analysis

Although we observed significant age differences in FC similarity using a whole brain parcellation scheme, the pattern of findings for global segregation were somewhat different from that of local EMN segregation. YA showed higher segregation during both rest and task states compared with OA, but task segregation was higher than rest segregation for both age groups. In addition, we observed a greater difference between rest versus task segregation in YA compared with OA. Thus, the finding of less segregation between (EMN) networks in response to an (EMN) task compared with rest appear to be specific to the networks involved in the task.

←

with older adults. ***G***, Younger adults showed a greater difference in rest versus task segregation compared with older adults. On each box, the central mark indicates the median, and the bottom and top edges of the box indicate the 25th and 75th percentiles, respectively. The whiskers extend to the most extreme data points not considered outliers. FTP = 18F-Flortaucipir; SUVR = Standard Uptake Value Ratio; EMN = episodic memory network.

Importantly, we did not observe any significant associations between FC similarity with either AD pathology or task performance in this whole brain analysis. This suggests that whereas the effects of age on FC similarity may represent a more global phenomenon, the link between FC similarity with AD pathology and object-related memory ability may reflect more local effects confined to this memory network. More broadly, they suggest that FC reconfiguration efficiency is not a global phenomenon, but rather reflects the efficiency of functional networks that are particularly important for a given task with privileged influences on performance of that task.

Limitations

An important limitation of this study is that our measure of FC similarity depends on the comparison of two BOLD scans (i.e., rest vs task) that were collected using different parameters and durations. These methodological differences will likely have different susceptibilities to distortion. Because of both issues, OA will likely have greater distortion compared with younger adults. However, it is important to point out that, although the acquisition parameters between rest and task scans were different, these differences were identical for both age groups. In terms of age differences in atrophy and motion, we found that neither EMN GM volume nor motion ($ps > 0.05$; see Table 2-Table 4) affected the relationships between FC similarity with age, pathology, or behavior when we included them in our regressions. This suggests that distortion differences between the two scans does not have a major effect on these findings.

Another limitation is the different correlational methods used during first-level analysis for local (EMN) versus global effects. Semi-partial correlations were used to assess regional EMN FC because we wanted to determine the unique variance of each unilateral seed, while controlling for the variance of all other seed regions entered in the same model. In contrast, we used bivariate correlations for calculating global FC because there were too many ROIs (264) to use semi-partial correlations. We observed the same age differences in FC similarity using bivariate correlations instead of semi-partial correlations ($t = 4.4$, $p < 0.001$). However, we did not observe the same relationships between FC similarity with pathology or behavior ($ps > 0.05$), suggesting that these control results may be driven by the methodological approach rather than by a global versus local distinction.

In conclusion, taken together, the findings from this study link AD pathology to disruption of the functional architecture of a vulnerable episodic memory brain network during rest and (memory) task states in OA. They also suggest that memory decline in some OA may be influenced by the extent of change in the functional architectures between rest and task demands. Overall, dynamic FC changes from rest to task may be a novel mechanism by which aging and AD pathology impacts cognition.

References

Adams JN, Maass A, Harrison TM, Baker SL, Jagust WJ (2019) Cortical tau deposition follows patterns of entorhinal functional connectivity in aging. Elife 8:e49132.

Baker SL, Lockhart SN, Price JC, He M, Huesman RH, Schonhaut D, Faria J, Rabinovici G, Jagust WJ (2017a) Reference tissue–based kinetic evaluation of 18F-AV-1451 for tau imaging. J Nucl Med 58:332–338.

Baker SL, Maass A, Jagust WJ (2017b) Considerations and code for partial volume correcting 18F]-AV-1451 tau PET data. Data Brief 15:648–657.

Behzadi Y, Restom K, Liau J, Liu TT (2007) A component based noise correction method (CompCor) for BOLD and perfusion based fMRI. Neuroimage 37:90–101.

Berron D, Neumann K, Maass A, Schütze H, Fliessbach K, Kiven V, Jessen F, Sauvage M, Kumaran D, Düzel E (2018) Age-related functional changes in domain-specific medial temporal lobe pathways. Neurobiol Aging 65:86–97.

Berron D, van Westen D, Ossenkoppele R, Strandberg O, Hansson O (2020) Medial temporal lobe connectivity and its associations with cognition in early Alzheimer's disease. Brain 143:1233–1248.

Bullmore E, Sporns O (2012) The economy of brain network organization. Nat Rev Neurosci 13:336–349.

Burke SN, Wallace JL, Hartzell AL, Nematollahi S, Plange K, Barnes CA (2011) Age-associated deficits in pattern separation functions of the perirhinal cortex: a cross-species consensus. Behav Neurosci 125:836–847.

Cassady KE, Adams JN, Chen X, Maass A, Harrison TM, Landau S, Baker S, Jagust W (2021) Alzheimer's pathology is associated with dedifferentiation of intrinsic functional memory networks in aging. Cereb Cortex 31:4781–4793.

Chan MY, Park DC, Savalia NK, Petersen SE, Wig GS (2014) Decreased segregation of brain systems across the healthy adult lifespan. Proc Natl Acad Sci U S A 111:E4997–E5006.

Chen X, Cassady KE, Adams JN, Harrison TM, Baker SL, Jagust WJ (2021) Regional tau effects on prospective cognitive change in cognitively normal older adults. J Neurosci 41:366–375.

Cohen JR, D'Esposito M (2016) The segregation and integration of distinct brain networks and their relationship to cognition. J Neurosci 36:12083–12094.

Cole MW, Bassett DS, Power JD, Braver TS, Petersen SE (2014) Intrinsic and task-evoked network architectures of the human brain. Neuron 83:238–251.

Cole MW, Ito T, Schultz D, Mill R, Chen R, Cocuzza C (2019) Task activations produce spurious but systematic inflation of task functional connectivity estimates. Neuroimage 189:1–18.

de Calignon A, Polydoro M, Suárez-Calvet M, William C, Adamowicz DH, Kopeikina KJ, Pitstick R, Sahara N, Ashe KH, Carlson GA, Spires-Jones TL, Hyman BT (2012) Propagation of tau pathology in a model of early Alzheimer's disease. Neuron 73:685–697.

Fan L, Li H, Zhuo J, Zhang Y, Wang J, Chen L, Yang Z, Chu C, Xie S, Laird AR, Fox PT, Eickhoff SB, Yu C, Jiang T (2016) The human Brainnetome atlas: a new brain atlas based on connectional architecture. Cereb Cortex 26:3508–3526.

Franzmeier N, Rubinski A, Neitzel J, Kim Y, Damm A, Na DL, Kim HJ, Lyoo CH, Cho H, Finsterwalder S, Duering M, Seo SW, Ewers M; Alzheimer's Disease Neuroimaging Initiative (2019) Functional connectivity associated with tau levels in ageing, Alzheimer's, and small vessel disease. Brain 142:1093–1107.

Haier RJ, Siegel BV, Nuechterlein KH, Hazlett E, Wu JC, Paek J, Browning HL, Buchsbaum MS (1988) Cortical glucose metabolic rate correlates of abstract reasoning and attention studied with positron emission tomography. Intelligence 12:199–217.

Harrison TM, Maass A, Adams JN, Du R, Baker SL, Jagust WJ (2019) Tau deposition is associated with functional isolation of the hippocampus in aging. Nat Commun 10:4900.

Hedden T, Gabrieli JDE (2004) Insights into the ageing mind: a view from cognitive neuroscience. Nat Rev Neurosci 5:87–96.

Hughes C, Faskowitz J, Cassidy BS, Sporns O, Krendl AC (2020) Aging relates to a disproportionately weaker functional architecture of brain networks during rest and task states. Neuroimage 209:116521.

Lemieux L, Salek-Haddadi A, Lund TE, Laufs H, Carmichael D (2007) Modelling large motion events in fMRI studies of patients with epilepsy. Magn Reson Imaging 25:894–901.

Logan J, Fowler JS, Volkow ND, Wang GJ, Ding YS, Alexoff DL (1996) Distribution volume ratios without blood sampling from graphical analysis of PET data. J Cereb Blood Flow Metab 16:834–840.

Maass A, Landau S, Baker SL, Horng A, Lockhart SN, La Joie R, Rabinovici GD, Jagust WJ; Alzheimer's Disease Neuroimaging Initiative (2017) Comparison of multiple tau-PET measures as biomarkers in aging and Alzheimer's disease. Neuroimage 157:448–463.

Maass A, Berron D, Harrison TM, Adams JN, La Joie R, Baker S, Mellinger T, Bell RK, Swinnerton K, Inglis B, Rabinovici GD, Düzel E, Jagust WJ (2019) Alzheimer's pathology targets distinct memory networks in the ageing brain. Brain 142:2492–2509.

Monteiro TS, King BR, Zivari Adab H, Mantini D, Swinnen SP (2019) Age-related differences in network flexibility and segregation at rest and during motor performance. Neuroimage 194:93–104.

Mormino EC, Brandel MG, Madison CM, Rabinovici GD, Marks S, Baker SL, Jagust WJ (2012) Not quite PIB-positive, not quite PIB-negative: slight PIB elevations in elderly normal control subjects are biologically relevant. Neuroimage 59:1152–1160.

Nelson PT, et al. (2012) Correlation of Alzheimer disease neuropathologic changes with cognitive status: a review of the literature. J Neuropathol Exp Neurol 71:362–381.

Power JD, Mitra A, Laumann TO, Snyder AZ, Schlaggar BL, Petersen SE (2014) Methods to detect, characterize, and remove motion artifact in resting state fMRI. Neuroimage 84:320–341.

Ranganath C, Ritchey M (2012) Two cortical systems for memory-guided behaviour. Nat Rev Neurosci 13:713–726.

Reagh ZM, Ho HD, Leal SL, Noche JA, Chun A, Murray EA, Yassa MA (2016) Greater loss of object than spatial mnemonic discrimination in aged adults. Hippocampus 26:417–422.

Rousset OG, Ma Y, Evans AC (1998) Correction for partial volume effects in PET: principle and validation. J Nucl Med 39:904–911.

Schultz DH, Cole MW (2016) Higher intelligence is associated with less task-related brain network reconfiguration. J Neurosci 36:8551–8561.

Shine JM, Bissett PG, Bell PT, Koyejo O, Balsters JH, Gorgolewski KJ, Moodie CA, Poldrack RA (2016) The dynamics of functional brain networks: integrated network states during cognitive task performance. Neuron 92:544–554.

Thomas Yeo BT, Krienen FM, Sepulcre J, Sabuncu MR, Lashkari D, Hollinshead M, Roffman JL, Smoller JW, Zöllei L, Polimeni JR, Fischl B, Liu H, Buckner RL (2011) The organization of the human cerebral cortex estimated by intrinsic functional connectivity. J Neurophysiol 106:1125–1165.

Villeneuve S, et al. (2015) Existing Pittsburgh Compound-B positron emission tomography thresholds are too high: statistical and pathological evaluation. Brain 138:2020–2033.

Vogel JW, Iturria-Medina Y, Strandberg OT, Smith R, Levitis E, Evans AC, Hansson O; Alzheimer's Disease Neuroimaging Initiative; Swedish BioFinder Study (2020) Spread of pathological tau proteins through communicating neurons in human Alzheimer's disease. Nat Commun 11:2612.

Wu JW, Hussaini SA, Bastille IM, Rodriguez GA, Mrejeru A, Rilett K, Sanders DW, Cook C, Fu H, Boonen RACM, Herman M, Nahmani E, Emrani S, Figueroa YH, Diamond MI, Clelland CL, Wray S, Duff KE (2016) Neuronal activity enhances tau propagation and tau pathology in vivo. Nat Neurosci 19:1085–1092.

Yassa MA (2014) Ground zero in Alzheimer's disease. Nat Neurosci 17:146–147.

Zar JH (1996) Biostatistical analysis. Hoboken: Prentice Hall.